

Structural Variations of Potassium Aryloxides

Timothy J. Boyle,* Nicholas L. Andrews, Mark A. Rodriguez, Charles Campana,† and Timothy Yiu

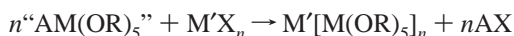
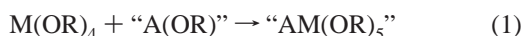
Advanced Materials Laboratory, Sandia National Laboratories, 1001 University Boulevard SE, Albuquerque, New Mexico 87106, and BRUKER AXS Inc., 5465 East Cheryl Parkway, Madison, Wisconsin 53711-5373

Received February 27, 2003

A series of potassium aryloxides (KOAr) were isolated from the reaction of a potassium amide (KN(SiMe₃)₂) and the desired substituted phenoxide (oMP, 2-methyl; oPP, 2-*iso*-propyl; oBP, 2-*tert*-butyl; DMP, 2,6-di-methyl; DIP, 2,6-di-*iso*-propyl; DBP, 2,6-di-*tert*-butyl) in tetrahydrofuran (THF) or pyridine (py) as the following: {[K(μ_4 -oMP)(THF)][K(μ_3 -oMP)]₅]_∞ (1), {[K₆(η^6 , μ_3 -oMP)₄(η^6 , μ_4 -oMP)₂(py)₄]·[K₆(η^6 , μ_3 -oMP)₆(η^6 -py)₄]_∞ (2), [K(μ_3 -oPP)]₄(THF)₃ (3), {K₄(η^6 , μ_3 -oPP)₂(μ_3 -oPP)₂(py)₃]_∞ (4), [K(μ_3 -oBP)(THF)]₆ (5), {K₆(η^6 , μ_3 -oBP)₂(μ_3 -oBP)₄(py)₄]_∞ (6), {K₃(η^6 , μ_3 -DMP)₂(μ -DMP)(THF)]_∞ (7), {[K(η^6 , μ -DMP)(py)]₂]_∞ (8), {K(η^6 , μ -DIP)]_∞ (9), {K(η^6 , μ -DBP)]_∞ (10). Further exploration of the aryl interactions led to the investigation of the diphenylethoxide (DPE) derivative which was isolated as [K(μ_3 -DPE)(THF)]₄ (11) or [K(μ_3 -DPE)(py)]₄·py₂ (12) depending on the solvent used. In general, the less sterically demanding ligands (oMP, oPP, oBP, and DMP) were solvated polymeric species; however, increasing the steric bulk (DIP and DBP) led to unsolvated polymers and not discrete molecules. For most of this novel family of compounds, the K atoms were π -bound to the aryl rings of the neighboring phenoxide derivatives to fill their coordination sites. The synthesis and characterization of these compounds are described in detail.

Introduction

Metal alkoxides are excellent precursors to ceramic oxide materials. Heteronuclear species with the desired stoichiometry, or “single-source” precursors to complex ceramic materials, are of continued interest to simplify the production of higher quality materials. In order to generate these mixed-metal precursors, metathesis reactions involving alkali metal alkoxides [A(OR)] are often thought to be a viable means to systematically synthesize these types of compounds (eq 1).



However, the “simplistically” written “A(OR)” precursors are often more complex than is typically realized,^{1–16} and

* To whom correspondence should be addressed. E-mail: tjboyle@Sandia.gov. Phone: (505) 272-7625. Fax: (505) 272-7336.

† BRUKER AXS Inc.

- Beck, G.; Hitchcock, P. B.; Lappert, M. F.; Mackinnon, I. A. *J. Chem. Soc., Chem. Commun.* **1989**, 1312.
- Cetinkaya, B.; Gumrukcu, I.; Lappert, M. F.; Atwood, J. L.; Shakir, R. *J. Am. Chem. Soc.* **1980**, *102*, 2086.
- Chisholm, M. H.; Drake, S. R.; Naiini, A. A.; Streib, W. E. *Polyhedron* **1991**, *10*, 805.

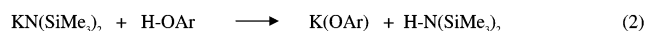
unfortunately, retention of the alkali metal or halide is often observed. To understand this phenomenon, we investigated the structural aspects of the “ATi(OR)₅” (Li, Na, K) family of compounds. The alkali metal centers were found to be unavailable for exchange due to the sterically encumbered nature of these atoms within these compounds.¹⁷

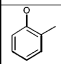
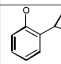
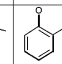
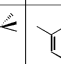
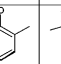
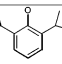
In further studies to generate an accessible metathesizable cation, we structurally characterized a wide range of lithium aryloxides in a variety of solvents, [Li(OAr(solv))]_n.¹⁸ It was

- Goldfuss, B.; Schleyer, P. V. R.; Hampel, F. *J. Am. Chem. Soc.* **1996**, *118*, 12183.
- Goldfuss, B.; Schleyer, P. V. R.; Hampel, F. *J. Am. Chem. Soc.* **1997**, *119*, 1072.
- Huffman, J. C.; Geerts, R. L.; Caulton, K. G. *J. Crystallogr. Spectrosc. Res.* **1984**, *14*, 541.
- Hvoslef, J.; Hope, H.; Murray, B. D.; Power, P. P. *J. Chem. Soc., Chem. Commun.* **1983**, 1438.
- Jackmann, L. M.; Debrosse, C. W. *J. Am. Chem. Soc.* **1983**, *105*, 4177.
- Jackmann, L. M.; Smith, B. D. *J. Am. Chem. Soc.* **1988**, *110*, 3829.
- Jackmann, L. M.; Cizmeciyan, D.; Williard, P. G.; Nichols, M. A. *J. Am. Chem. Soc.* **1993**, *115*, 6262.
- Kociok-Kohn, G.; Pickardt, J.; Shumann, H. *Acta Crystallogr.* **1991**, *C47*, 2649.
- Thiele, K.; Goerls, H.; Seidel, W. Z. *Anorg. Allg. Chem.* **1998**, *624*, 1391.
- Williard, P. G.; Carpenter, G. B. *J. Am. Chem. Soc.* **1985**, *107*, 3345.
- Williard, P. G.; Carpenter, G. B. *J. Am. Chem. Soc.* **1986**, *108*, 462.
- Williard, P. G.; MacEwan, G. J. *J. Am. Chem. Soc.* **1989**, *111*, 7671.
- Wheatley, P. J. *J. Chem. Soc.* **1960**, 4270.
- Boyle, T. J.; Bradley, D. C.; Hampden-Smith, M. J.; Patel, A.; Ziller, J. W. *Inorg. Chem.* **1995**, *34*, 5893.

found that, by varying the steric bulk around the metal center as well as the Lewis basicity of the solvent, structures ranging from hexanuclear prisms to cubes to hexagons to squares could be isolated. It was therefore of interest to investigate the structure of the larger congener, potassium aryloxides [K(OAr)]. Furthermore, there are numerous reaction pathways, such as the Kolbe–Schmidt synthesis,¹⁹ that would benefit from knowing the structure of a series of K(OAr) compounds.²⁰

Surprisingly, there are only a few simple K(OAr) structures available in the literature:^{21,22} (a) $K_6(\text{OPh})_6(\text{HOPh})_3$,^{23,20} where HOPh = phenol, (b) $K_6(\text{TBOM})_2(\text{THF})_6 \cdot \text{THF}$ where TBOM- H_3 = tris(3,5-di-*tert*-butyl-2-oxyphenyl)methane and THF = tetrahydrofuran,²⁴ (c) K(quinolin-8-olate)bis(quinolin-8-oland),^{25,26} and (d) $(\eta^6\text{-}2\text{-BzPhO})(\eta^2\text{-}2\text{-BzPhOH})_2\text{K}(\text{OPh-}2\text{-Bz})$ where 2-BzPhOH = 2-benzylphenol.²⁷ Typically, the limited number of structurally characterized species is attributed to oligomerization that occurs due to the large cation size coupled with the small charge on the metal. The resulting reduced solubility makes it difficult to generate crystalline material. Bulky ligands, such as crown ethers, are often used to prevent this from occurring, and thus, the majority of crystalline K(OAr) species isolated utilize this ligand.^{21,22} Unfortunately, these structures lend little insight into the actual K atom position in K(OAr). On the basis of this lack of structural understanding and our interest in metathesizable species, we undertook the structural characterization of a series of K(OAr) species in the Lewis basic solvent THF or pyridine (py). The amide alcohol exchange (eq 2) was again¹⁸ used as the route to generate these precursors using the substituted phenoxide (oMP, 2-methyl; oPP, 2-*iso*-propyl; oBP, 2-*tert*-butyl; DMP, 2,6-di-methyl; DIP, 2,6-di-*iso*-propyl; DBP, 2,6-di-*tert*-butyl) as the alcohol in THF or py. The following compounds were synthesized



Abbreviations	oMP	oPP	oBP	DMP	DIP	DBP
Structure scheme						

and characterized as the following: $\{([\text{K}(\mu_4\text{-oMP})(\text{THF})][\text{K}(\mu_3\text{-oMP})])_5\}_\infty$ (**1**), $\{[\text{K}_6(\eta^6\mu_3\text{-oMP})_4(\eta^6\mu_4\text{-oMP})_2(\text{py})_4] \cdot [\text{K}_6(\eta^6\mu_3\text{-oMP})_6(\eta^6\text{-py})_4]\}_\infty$ (**2**), $[\text{K}(\mu_3\text{-oPP})]_4(\text{THF})_3$ (**3**),

- (18) Boyle, T. J.; Pedrotty, D. M.; Alam, T. M.; Vick, S. C.; Rodriguez, M. A. *Inorg. Chem.* **2000**, *39*, 5133.
 (19) Kolbe, H. J. *Prakt. Chem.* **1874**, *118*, 107.
 (20) Dinnebier, R. E.; Pink, M.; Sieler, J.; Norby, P.; Stephens, P. W. *Inorg. Chem.* **1998**, *37*, 4996.
 (21) Bradley, D. C.; Mehrotra, R. C.; Rothwell, I. P.; Singh, A. *Alkoxo and Aryloxo Derivatives of Metals*; Academic Press: San Diego, CA, 2001.
 (22) The Cambridge Crystallographic Data Centre, 12 Union Road, Cambridge CB2 1EZ, United Kingdom, www.ccdc.cam.ac.uk, was searched using ConQuest v 1.5 (November 2002).
 (23) Dinnebier, R. E.; Pink, M.; Sieler, J.; Stephens, P. W. *Inorg. Chem.* **1997**, *36*, 3398.
 (24) Dinger, M. B.; Scott, M. J. *Inorg. Chem.* **2000**, *39*, 1238.
 (25) Hughes, D. I.; Truter, M. R. *J. Chem. Soc., Dalton Trans.* **1979**, 250.
 (26) Hughes, D. I.; Truter, M. R. *J. Chem. Soc., Dalton Trans.* **1979**, 520.
 (27) Bryan, J. C.; Delmau, L. H.; Hay, B. P.; Nicholas, J. B.; Rogers, L. M.; Rogers, R. D.; Moyer, B. A. *Struct. Chem.* **1999**, *10*, 187.

$\{[\text{K}_4(\eta^6\mu_3\text{-oPP})_2(\mu_3\text{-oPP})_2(\text{py})_3]\}_\infty$ (**4**), $[\text{K}(\mu_3\text{-oBP})(\text{THF})]_6$ (**5**), $\{[\text{K}_6(\eta^6\mu_3\text{-oBP})_2(\mu_3\text{-oBP})_4(\text{py})_4]\}_\infty$ (**6**), $\{[\text{K}_3(\eta^6\mu_3\text{-DMP})_2(\mu\text{-DMP})(\text{THF})]\}_\infty$ (**7**), $\{[\text{K}(\eta^6\mu\text{-DMP})(\text{py})]_2\}_\infty$ (**8**), $\{[\text{K}(\eta^6\mu\text{-DIP})]\}_\infty$ (**9**), $\{[\text{K}(\eta^6\mu\text{-DBP})]\}_\infty$ (**10**). Further exploration of the aryl interactions led to the investigation of the diphenylethoxide (DPE) derivative which was isolated from the above reaction as $[\text{K}(\mu_3\text{-DPE})(\text{THF})]_4$ (**11**) and $[\text{K}(\mu_3\text{-DPE})(\text{py})]_4(\text{py})_2$ (**12**). The synthesis and characterization of these compounds are described in detail.

Experimental Section

All described compounds were handled with rigorous exclusion of air and water using standard Schlenk line and glovebox techniques. All solvents were purchased from Aldrich (99.99%, sure-seal bottle), opened, and used as received in a glovebox under an argon atmosphere. The following chemicals were used as received (Aldrich): $\text{KN}(\text{SiMe}_3)_2$ (referred to as KNR_2), H-oMP, H-oPP, H-oBP, H-DMP, H-DIP, H-DBP, and H-DPE.

FT-IR data were obtained on a Bruker Vector 22 instrument using KBr pellets under an atmosphere of flowing nitrogen. Elemental analysis was performed on a Perkin-Elmer 2400 CHN-S/O elemental analyzer. All NMR samples were prepared from dried crystalline materials that were handled and stored under an argon atmosphere, and spectra were obtained on a Bruker DMX400 spectrometer at 399.87 and 100.54 MHz for ^1H and ^{13}C experiments, respectively. A 5 mm broadband probe was used for all experiments. ^1H NMR spectra were obtained using a direct single pulse excitation, with a 10 s recycle delay and 16 scan average. The $^{13}\text{C}\{^1\text{H}\}$ NMR spectra were obtained using a WALTZ-16 composite pulse ^1H decoupling, a 5 s recycle delay, and a $\pi/4$ pulse excitation.

General Synthesis. Due to the similarity of synthetic procedures, a general description is presented. After KNR_2 was dissolved in either THF or py, the appropriate HOAr was added and the reaction stirred for 12 h. After this time, the volume of the clear reaction mixture was significantly reduced by rotary evaporation and then placed in a freezer at -35°C or was allowed to slowly evaporate at glovebox temperatures. X-ray quality crystals were isolated for each reaction mixture.

$\{([\text{K}(\mu_4\text{-oMP})(\text{THF})][\text{K}(\mu_3\text{-oMP})])_5\}_\infty$ (**1**). H-oMP (0.278 g, 2.57 mmol), $\text{KN}(\text{SiMe}_3)_2$ (0.500 g, 2.51 mmol), and 10 mL of THF were used. Yield 3.36 g (73.7%). FTIR (KBr, cm^{-1}) 2995(m), 1586(s), 1546(w), 1491(s), 1471(s), 1439(s), 1330(s), 1301(s), 1248(w), 1175(w), 1149(w), 1107(w), 1059(w), 1041(m), 972(w), 917(w), 859(m), 760(m), 720(m), 588(w), 541(w). ^1H NMR (399.872 MHz, THF- d_8): δ 6.71 (1.0H, d, $\text{OC}_6\text{H}_4\text{Me}$, $J_{\text{H-H}} = 3.4$ Hz), 6.69 (1.1H, t, $\text{OC}_6\text{H}_4\text{Me}$, $J_{\text{H-H}} = 3.75$), 6.26 (1.0H, d, $\text{OC}_6\text{H}_4\text{Me}$, $J_{\text{H-H}} = 3.8$ Hz), 5.99 (1.0H, t, $\text{OC}_6\text{H}_4\text{Me}$, $J_{\text{H-H}} = 3.5$), 2.03 (3.1H, s, $\text{OC}_6\text{H}_4\text{Me}$). Anal. Calcd for $\text{C}_{72}\text{H}_{88}\text{K}_8\text{O}_{12}$: C, 59.30; H, 6.08. Found: C, 57.33; H, 5.91.

$\{[\text{K}_6(\eta^6\mu_3\text{-oMP})_4(\eta^6\mu_4\text{-oMP})_2(\text{py})_4] \cdot [\text{K}_6(\eta^6\mu_3\text{-oMP})_6(\eta^6\text{-py})_4]\}_\infty$ (**2**). H-oMP (0.272 g, 2.52 mmol), $\text{KN}(\text{SiMe}_3)_2$ (0.500 g, 2.51 mmol), and 10 mL of py were used. Yield 2.52 g (84.2%). FTIR (KBr, cm^{-1}) 2993(m), 1585(s), 1548(w), 1489(s), 1472(s), 1439(s), 1316(s), 1297(s), 1248(m), 1175(m), 1150(m), 1108(m), 1043(m), 996(w), 859(m), 763(s), 723(m), 703(m), 608(w), 540(w). ^1H NMR (399.872 MHz, py- d_5): δ 7.24 (1.1H, d, $\text{OC}_6\text{H}_4\text{Me}$, $J_{\text{H-H}} = 3.2$ Hz), 7.13 (1.0H, t, $\text{OC}_6\text{H}_4\text{Me}$, $J_{\text{H-H}} = 3.7$ Hz), 6.95 (1.0H, d, $\text{OC}_6\text{H}_4\text{Me}$, $J_{\text{H-H}} = 3.8$ Hz), 6.51 (1.0H, t, $\text{OC}_6\text{H}_4\text{Me}$, $J_{\text{H-H}} = 3.5$ Hz), 2.35 (3.0H, s, $\text{OC}_6\text{H}_4\text{Me}$). Anal. Calcd for $\text{C}_{62}\text{H}_{62}\text{K}_6\text{N}_4\text{O}_6$: C, 62.38; H, 5.23; N, 4.69. Found: C, 57.66; H, 5.15; N, 2.00.

[K(μ_3 -oPP)]₄(THF)₃ (3). H-oPP (0.348 g, 2.56 mmol), KN(SiMe₃)₂ (0.500 g, 2.51 mmol), and 10 mL of THF were used. Yield 1.86 g (81.3%). FTIR (KBr, cm⁻¹) 2959(s), 2864(m), 1584(s), 1475(s), 1448(s), 1382(w), 1360(w), 1338(m), 1313(s), 1299(s), 1278(m), 1233(w), 1140(m), 1111(w), 1073(w), 1033(m), 927(w), 892(w), 840(m), 770(m), 742(m), 713(w), 590(w), 528(w). ¹H NMR (399.872 MHz, THF-*d*₈): δ 6.83 (1.0H, d, OC₆H₄CHMe₂, *J*_{H-H} = 3.4 Hz), 6.68 (1.0H, t, OC₆H₄CHMe₂, *J*_{H-H} = 3.75 Hz), 6.27 (1.0H, d, OC₆H₄CHMe₂, *J*_{H-H} = 3.8 Hz), 6.08 (1.0H, t, OC₆H₄CHMe₂, *J*_{H-H} = 3.7 Hz), 3.26 (1.0H, sept, *J*_{H-H} = 3.4 Hz), 1.19 (6.0H, d, OC₆H₄CHMe₂, *J*_{H-H} = 3.6 Hz). Anal. Calcd for C₄₈H₆₈K₄O₇: C, 63.11; H, 7.50; N, 6.13. Found: C, 61.25; H, 6.67.

{K(η^6 , μ_3 -oPP)₂(μ_3 -oPP)₂(py)₃}}_∞ (4). H-oPP (0.346 g, 2.54 mmol), KN(SiMe₃)₂ (0.500 g, 2.51 mmol), and 10 mL of py were used. Yield 1.84 g (78.5%). FTIR (KBr, cm⁻¹) 2959(s), 2863(m), 1584(s), 1475(s), 1439(s), 1339(m), 1312(s), 1299(s), 1274(m), 1233(w), 1142(m), 1073(w), 1032(m), 926(w), 892(w), 840(m), 768(m), 746(m), 703(m), 590(w), 527(w). ¹H NMR (399.872 MHz, py-*d*₅): δ 7.29 (1.0H, d, OC₆H₄CHMe₂, *J*_{H-H} = 3.6 Hz), 7.12 (1.0H, t, OC₆H₄CHMe₂, *J*_{H-H} = 3.2 Hz), 7.01 (1.0H, d, OC₆H₄CHMe₂, *J*_{H-H} = 4.0 Hz), 6.61 (1.0H, t, OC₆H₄CHMe₂, *J*_{H-H} = 3.5 Hz), 3.74 (1.0H, sept, OC₆H₄CHMe₂, *J*_{H-H} = 3.4 Hz), 1.23 (6.0H, d, OC₆H₄CHMe₂, *J*_{H-H} = 3.4 Hz). Anal. Calcd for C₅₁H₅₉K₄N₃O₄: C, 65.55; H, 6.36; N, 5.99. Found: C, 62.84; H, 6.46; N, 4.07.

[K(μ_3 -oBP)(THF)]₆ (5). H-oBP (0.384 g, 2.56 mmol), KN(SiMe₃)₂ (0.500 g, 2.51 mmol), and 10 mL of THF were used. Yield 3.46 g (88.3%). FTIR (KBr, cm⁻¹) 3084(m), 3043(m), 2950(s), 2865(s), 1584(s), 1553(m), 1473(s), 1435(s), 1383(m), 1343(m), 1311(s), 1267(s), 1229(m), 1199(m), 1152(m), 1121(s), 1059(s), 1048(s), 926(m), 898(m), 863(s), 847(m), 815(m), 767(m), 745(s), 680(w), 584(m), 551(m), 518(m). ¹H NMR (399.872 MHz, THF-*d*₈): δ 6.86 (1.0H, d, OC₆H₄CMe₃, *J*_{H-H} = 3.8 Hz), 6.67 (0.9H, t, OC₆H₄CMe₃, *J*_{H-H} = 3.7), 6.23 (0.9H, d, OC₆H₄CMe₃, *J*_{H-H} = 3.8 Hz), 5.96 (0.9H, t, OC₆H₄CMe₃, *J*_{H-H} = 3.3 Hz), 1.42 (8.5, s, OC₆H₄CMe₃). Anal. Calcd for C₈₄H₁₂₆K₆O₁₂: C, 64.57; H, 8.13. Found: C, 63.81; H, 8.16.

{K(η^6 , μ_3 -oBP)₂(μ_3 -oBP)₄(py)₄}}_∞ (6). H-oBP (0.386 g, 2.57 mmol), KN(SiMe₃)₂ (0.500 g, 2.51 mmol), and 10 mL of py were used. Yield 3.11 g (85.6%). FTIR (KBr, cm⁻¹) 3081(w), 3038(m), 3005(m), 2989(s), 2964(s), 2946(s), 2905(s), 2850(m), 1609(w), 1587(s), 1578(s), 1552(m), 1473(s), 1439(s), 1382(m), 1344(m), 1328(s), 1308(s), 1284(m), 1228(m), 1199(m), 1149(m), 1119(m), 1074(w), 1045(m), 1031(m), 996(m), 925(w), 884(w), 863(s), 848(m), 814(m), 770(m), 750(s), 703(s), 676(w), 609(w), 583(w), 550(w), 518(w). ¹H NMR (399.872 MHz, py-*d*₅): δ 7.42 (1.0H, d, OC₆H₄CMe₃, *J*_{H-H} = 3.7 Hz), 7.19 (1.0H, t, OC₆H₄CMe₃, *J*_{H-H} = 3.7 Hz), 6.97 (1.0H, d, OC₆H₄CMe₃, *J*_{H-H} = 4.0 Hz), 6.57 (1.0H, t, OC₆H₄CMe₃, *J*_{H-H} = 3.6 Hz), 1.68 (9.0H, s, OC₆H₄CMe₃). Anal. Calcd for C₈₀H₉₈K₆N₄O₆: C, 66.44; H, 6.83; N, 3.87. Found: C, 64.75; H, 6.68; N, 3.69.

{K₃(η^6 , μ_3 -DMP)₂(μ -DMP)(THF)}_∞ (7). H-DMP (0.308 g, 2.52 mmol), KN(SiMe₃)₂ (0.500 g, 2.51 mmol), and 10 mL of THF were used. Yield 1.02 g (74.1%). FTIR (KBr, cm⁻¹) 3058(m), 2960(s), 2846(s), 1829(w), 1790(w), 1651(w), 1585(s), 1549(w), 1480(s), 1424(s), 1366(s), 1338(m), 1321(s), 1310(s), 1291(s), 1233(m), 1175(w), 1152(w), 1089(s), 1053(m), 973(w), 936(w), 910(m), 892(w), 846(s), 762(s), 680(m), 496(s). ¹H NMR (399.872 MHz, THF-*d*₈): δ 6.66 (2.0H, d, OC₆H₃Me₂, *J*_{H-H} = 3.4 Hz), 5.89 (1.0H, t, OC₆H₃Me₂, *J*_{H-H} = 3.6 Hz), 2.07 (6.1H, s, OC₆H₃Me₂). Anal. Calcd for C₂₈H₃₅K₃O₄: C, 60.83; H, 6.38. Found: C, 57.20; H, 5.90.

{[K(η^6 , μ -DMP)(py)]₂}}_∞ (8). H-DMP (0.306 g, 2.50 mmol), KN(SiMe₃)₂ (0.500 g, 2.51 mmol), and 10 mL of py were used. Yield 0.99 g (82.0%). FTIR (KBr, cm⁻¹) 2963(s), 1585(s), 1478(s), 1467(s), 1440(s), 1426(s), 1365(w), 1322(m), 1087(m), 1031(w), 994(w), 910(w), 846(m), 759(m), 745(m), 704(m), 680(w), 607(w), 497(w). ¹H NMR (399.872 MHz, py-*d*₅): δ 7.25 (2.0H, d, OC₆H₃Me₂, *J*_{H-H} = 3.6 Hz), 6.50 (1.0H, t, OC₆H₃Me₂, *J*_{H-H} = 3.5 Hz), 2.49 (6.2H, s, OC₆H₃Me₂). Anal. Calcd for C₂₆H₂₈K₂N₂O₂: C, 65.23; H, 5.90; N, 5.85. Found: C, 63.15; H, 5.95; N, 5.22.

{K(η^6 , μ -DIP)}_∞ (9). (A) H-DIP (0.462 g, 2.59 mmol), KN(SiMe₃)₂ (0.512 g, 2.57 mmol), and 10 mL of THF were used. Yield 0.45 g (81.4%). (B) H-DIP (0.494 g, 2.77 mmol), KN(SiMe₃)₂ (0.542 g, 2.72 mmol), and 10 mL of py were used. Yield 0.49 g (83.2%). FTIR (KBr, cm⁻¹) 2953(s), 2864(m), 1582(m), 1425(s), 1374(m), 1346(m), 1281(m), 1261(w), 1154(w), 1133(w), 1106(w), 1038(w), 949(w), 883(w), 840(m), 801(w), 763(m), 675(w), 525(w). ¹H NMR (399.872 MHz, THF-*d*₈): δ 6.68 (2.0H, d, OC₆H₃(CHMe₂)₂, *J*_{H-H} = 3.6 Hz), 6.02 (1.0H, t, OC₆H₃(CHMe₂)₂, *J*_{H-H} = 3.7 Hz), 3.53 (2.4H, sept, OC₆H₃(CHMe₂)₂, *J*_{H-H} = 3.5 Hz), 1.13 (12.4H, d, OC₆H₃(CHMe₂)₂, *J*_{H-H} = 3.6 Hz). ¹H NMR (399.872 MHz, py-*d*₅): δ 7.25 (2.0H, d, OC₆H₃(CHMe₂)₂, *J*_{H-H} = 3.6 Hz), 6.66 (1.0H, t, OC₆H₃(CHMe₂)₂, *J*_{H-H} = 3.7 Hz), 4.03 (2.0H, sept, OC₆H₃(CHMe₂)₂, *J*_{H-H} = 3.4 Hz), 1.32 (12.2H, d, OC₆H₃(CHMe₂)₂, *J*_{H-H} = 3.6 Hz). Anal. Calcd for C₁₂H₁₇KO: C, 66.62; H, 7.92. Found: C, 66.07; H, 7.90.

{K(η^6 , μ -DBP)}_∞ (10). (A) H-DBP (0.520 g, 2.52 mmol), KN(SiMe₃)₂ (0.500 g, 2.51 mmol), and 10 mL of THF were used. Yield 0.54 g (88.4%). (B) H-DBP (0.518 g, 2.51 mmol), KN(SiMe₃)₂ (0.500 g, 2.51 mmol), and 10 mL of py were used. Yield 0.53 g (86.6%). FTIR (KBr, cm⁻¹) 3012(m), 2956(s), 2865(m), 1574(w), 1459(w), 1414(s), 1375(m), 1354(m), 1299(s), 1276(w), 1254(w), 1199(w), 1143(w), 1095(m), 880(w), 855(w), 812(w), 757(s), 628(w), 527(w). ¹H NMR (399.872 MHz, THF-*d*₈): δ 6.73 (2.0H, d, OC₆H₃(CMe₃)₂, *J*_{H-H} = 3.6 Hz), 5.79 (0.9H, t, OC₆H₃(CMe₃)₂, *J*_{H-H} = 3.8 Hz), 1.39 (18.2H, s, OC₆H₃(CMe₃)₂). Anal. Calcd for C₁₄H₂₁KO: C, 68.80; H, 8.66. Found: C, 69.21; H, 8.63.

[K(μ_3 -DPE)(THF)]₄ (11). H-DPE (0.996 g, 5.02 mmol), KN(SiMe₃)₂ (1.00 g, 5.01 mmol), and 10 mL of THF were used. Yield 4.88 g (78.9%). FTIR (KBr, cm⁻¹) 3076(m), 3014(m), 2954(s), 2854(m), 1593(m), 1487(s), 1442(s), 1396(w), 1345(m), 1293(w), 1218(m), 1185(s), 1164(m), 1129(s), 1110(m), 1058(s), 1024(s), 934(s), 909(m), 827(w), 776(s), 759(s), 603(s), 623(s), 585(m), 560(w). ¹H NMR (399.872 MHz, THF-*d*₈): δ 7.32 (4.0H, d, OCMe(C₆H₅)₂, *J*_{H-H} = 3.6 Hz), 7.10 (4.1H, t, OCMe(C₆H₅)₂, *J*_{H-H} = 3.8 Hz), 6.96 (2.0H, t, OCMe(C₆H₅)₂, *J*_{H-H} = 3.6 Hz), 1.71 (3.0H, s, OCMe(C₆H₅)₂). ¹H NMR (399.872 MHz, THF-*d*₈): δ 7.32 (4.0H, d, OCMe(C₆H₅)₂, *J*_{H-H} = 3.6 Hz), 7.10 (4.1H, t, OCMe(C₆H₅)₂, *J*_{H-H} = 3.8 Hz), 6.96 (2.0H, t, OCMe(C₆H₅)₂, *J*_{H-H} = 3.6 Hz), 1.71 (3.0H, s, OCMe(C₆H₅)₂). Anal. Calcd for C₇₂H₈₄K₄O₈: C, 70.09; H, 6.86. Found: C, 68.63; H, 5.95.

[K(μ_3 -DPE)(py)]₄·py₂ (12). H-DPE (0.520 g, 2.62 mmol), KN(SiMe₃)₂ (0.518 g, 2.60 mmol), and 10 mL of py were used. Yield 2.93 g (91.3%). FTIR (KBr, cm⁻¹) 3075(m), 3053(m), 3014(m), 2950(s), 2855(w), 1586(m), 1486(m), 1440(s), 1398(w), 1348(w), 1292(w), 1209(m), 1183(m), 1164(w), 1128(s), 1058(s), 1022(m), 993(w), 934(m), 913(m), 825(w), 776(m), 761(s), 748(m), 703(s), 623(m), 584(m), 563(w). ¹H NMR (399.872 MHz, py-*d*₅): δ 7.72 (4.0H, d, OCMe(C₆H₅)₂, *J*_{H-H} = 3.8 Hz), 7.28 (4.0H, t, OCMe(C₆H₅)₂, *J*_{H-H} = 3.8 Hz), 7.12 (2.0H, t, OCMe(C₆H₅)₂, *J*_{H-H} = 3.7 Hz), 1.93 (2.9H, s, OCMe(C₆H₅)₂). Anal. Calcd for C₈₆H₈₂K₄N₆O₄: C, 72.74; H, 5.82; N, 5.92. Found: C, 69.12; H, 5.85; N, 0.73.

Table 1. Data Collection Parameters for **1** and **2**

	1	2
chemical formula	C ₇₂ H ₈₈ K ₈ O ₁₂	C ₆₂ H ₆₂ K ₆ N ₄ O ₆
fw	1458.22	1193.76
temp (K)	168(2)	168(2)
space group	tetragonal <i>I</i> 4 ₁ / <i>a</i>	monoclinic <i>P</i> 2 ₁ / <i>c</i>
<i>a</i> (Å)	24.604(3)	13.538(6)
<i>b</i> (Å)	24.604(3)	26.327(11)
<i>c</i> (Å)	12.130(2)	17.208(7)
β (deg)		97.284(8)
<i>V</i> (Å ³)	7342.7(19)	6084(4)
<i>Z</i>	4	4
<i>D</i> _{calcd} (Mg/m ³)	1.319	1.303
μ(Mo Kα) (mm ⁻¹)	0.527	0.482
R1 ^a (%)	5.42	6.39
wR2 ^b (%)	16.61	10.71

^a R1 = $\sum ||F_o| - |F_c|| / \sum |F_o| \times 100$. ^b wR2 = $[\sum w(F_o^2 - F_c^2)^2 / \sum (w|F_o|^2)^2]^{1/2} \times 100$ for $[I < 2\sigma(I)]$.

General X-ray Crystal Structure Information.²⁸ Each crystal was mounted onto a thin glass fiber from a pool of Fluorolube and immediately placed under a liquid N₂ stream, on a Bruker AXS diffractometer. The radiation used was graphite monochromatized Mo Kα radiation ($\lambda = 0.7107$ Å). The lattice parameters were optimized from a least-squares calculation on carefully centered reflections. Lattice determination and data collection were carried out using SMART version 5.054 software. Data reduction was performed using SAINT version 6.01 software. The structure refinement was performed using XSHHELL 3.0 software. The data were corrected for absorption using the SADABS program within the SAINT software package.

Each structure was solved using direct methods. This procedure yielded the heavy atoms, along with a number of the C, N, and O atoms. Subsequent Fourier synthesis yielded the remaining C, N, and O atom positions. The hydrogen atoms were fixed in positions of ideal geometry and refined within the XSHHELL software. These idealized hydrogen atoms had their isotropic temperature factors fixed at 1.2 or 1.5 times the equivalent isotropic *U* of the C atoms to which they were bonded. The final refinement of each compound included anisotropic thermal parameters on all non-hydrogen atoms. Any problematic aspects of the structural solutions are listed in following paragraphs. Data collection parameters are given in Tables 1–6. Additional information concerning the data collection and final structural solutions of **1–12** can be found in the Supporting Information or by accessing CIF files through the Cambridge Crystal Data Centre.

[K(μ₃-oBP)(THF)]₆ (5). One restraint was used to fix the O6–C36 bond distance in the O6 THF to be equivalent to the O6–C42 bond length. This restraint helped stabilize the THF ligand.

{K(η⁶,μ-DIP)}_∞ (9). The structure refinement indicated a possible racemic twin; a twin command was included in the refinement to accommodate this observation and the absolute structure parameter refined to zero (0).

[K(μ₃-DPE)(py)]₄·py₂ (12). The structure was solved in the space group *P*4̄ using direct methods. This solution yielded the K, O, N, and some of the C atoms. This structure was determined to be merohedrally twinned, emulating the *P*4̄*m*2 space group. Addition of the twin law properly modeled the twin relationship in the *P*4̄ space group. Subsequent refinements yielded the remaining C atoms. There were four independent molecules of K₄(DPE)₄(py)₄ in the unit cell. Two were in the unit cell face, one located on the

Table 2. Data Collection Parameters for **3** and **4**

	3	4
chemical formula	C ₄₈ H ₆₈ K ₄ O ₇	C ₅₁ H ₅₉ K ₄ N ₃ O ₄
fw	913.42	934.41
temp (K)	168(2)	168(2)
space group	triclinic <i>P</i> 1̄	orthorhombic <i>P</i> 2 ₁ 2 ₁ 2 ₁
<i>a</i> (Å)	13.309(4)	16.348(8)
<i>b</i> (Å)	14.314(4)	17.500(8)
<i>c</i> (Å)	14.537(4)	17.999(9)
α (deg)	88.714(5)	
β (deg)	87.819(5)	
γ (deg)	64.566(5)	
<i>V</i> (Å ³)	2499.1(12)	5150(4)
<i>Z</i>	2	4
<i>D</i> _{calcd} (Mg/m ³)	1.214	1.205
μ(Mo Kα) (mm ⁻¹)	0.402	0.389
R1 ^a (%)	4.86	4.87
wR2 ^b (%)	11.67	8.46

^a R1 = $\sum ||F_o| - |F_c|| / \sum |F_o| \times 100$. ^b wR2 = $[\sum w(F_o^2 - F_c^2)^2 / \sum (w|F_o|^2)^2]^{1/2} \times 100$ for $[I < 2\sigma(I)]$.

Table 3. Data Collection Parameters for **5** and **6**

	5	6
chemical formula	C ₈₄ H ₁₂₆ K ₆ O ₁₂	C ₈₀ H ₉₈ K ₆ N ₄ O ₆
fw	1562.45	1446.22
temp (K)	168(2)	168(2)
space group	orthorhombic <i>Pbcz</i>	triclinic <i>P</i> 1̄
<i>a</i> (Å)	22.361(6)	12.059(4)
<i>b</i> (Å)	16.593(4)	13.910(4)
<i>c</i> (Å)	24.428(6)	14.008(5)
α (deg)		106.3354(6)
β (deg)		112.576(6)
γ (deg)		97.890(6)
<i>V</i> (Å ³)	9064(4)	2000.5(11)
<i>Z</i>	4	1
<i>D</i> _{calcd} (Mg/m ³)	1.145	1.200
μ(Mo Kα) (mm ⁻¹)	0.341	0.378
R1 ^a (%)	8.51	5.01
wR2 ^b (%)	22.74	10.41

^a R1 = $\sum ||F_o| - |F_c|| / \sum |F_o| \times 100$. ^b wR2 = $[\sum w(F_o^2 - F_c^2)^2 / \sum (w|F_o|^2)^2]^{1/2} \times 100$ for $[I < 2\sigma(I)]$.

Table 4. Data Collection Parameters for **7** and **8**

	7	8
chemical formula	C ₂₈ H ₃₅ K ₃ O ₄	C ₂₆ H ₂₈ K ₂ N ₂ O ₂
fw	552.86	478.70
temp (K)	168(2)	168(2)
space group	triclinic <i>P</i> 1̄	triclinic <i>P</i> 1̄
<i>a</i> (Å)	11.738(3)	11.485(2)
<i>b</i> (Å)	11.887(3)	11.844(2)
<i>c</i> (Å)	11.985(3)	12.012(2)
α (deg)	71.754(4)	117.927(3)
β (deg)	62.253(4)	108.854(3)
γ (deg)	74.888(4)	98.180(3)
<i>V</i> (Å ³)	1392.4(6)	1279.2(4)
<i>Z</i>	2	2
<i>D</i> _{calcd} (Mg/m ³)	1.319	1.243
μ(Mo Kα) (mm ⁻¹)	0.521	0.394
R1 ^a (%)	4.30	3.17
wR2 ^b (%)	9.43	8.12

^a R1 = $\sum ||F_o| - |F_c|| / \sum |F_o| \times 100$. ^b wR2 = $[\sum w(F_o^2 - F_c^2)^2 / \sum (w|F_o|^2)^2]^{1/2} \times 100$ for $[I < 2\sigma(I)]$.

cell corner and one located within the unit cell. Two disordered py molecules were observed as solvent within the lattice with symmetry generating an additional six more py solvent molecules. This results in a total of eight (py) solvent/cell or two per K₄(DPE)₄(py)₄ molecule. These py solvent molecules were successfully modeled

(28) The listed versions of SAINT, SMART, XSHHELL, and SADABS software from Bruker Analytical X-ray Systems Inc., 6300 Enterprise Lane, Madison, WI 53719, were used in analysis.

Table 5. Data Collection Parameters for **9** and **10**

	9	10
chemical formula	C ₁₂ H ₁₇ KO	C ₁₄ H ₂₁ KO
fw	216.36	244.41
temp (K)	168(2)	168(2)
space group	monoclinic <i>P2₁</i>	orthorhombic <i>P2₁2₁2₁</i>
<i>a</i> (Å)	9.698(4)	6.8267(11)
<i>b</i> (Å)	6.530(3)	12.316(2)
<i>c</i> (Å)	10.034(4)	16.190(3)
β (deg)	101	
<i>V</i> (Å ³)	622.9(4)	1361.3(4)
<i>Z</i>	2	4
<i>D</i> _{calcd} (Mg/m ³)	1.153	1.193
μ (Mo K α) (mm ⁻¹)	0.395	0.369
<i>R</i> ¹ (%)	3.38	3.66
w <i>R</i> ² (%)	7.41	7.20

$${}^a R1 = \frac{\sum ||F_o| - |F_c||}{\sum |F_o|} \times 100. {}^b wR2 = \frac{[\sum w(F_o^2 - F_c^2)^2]}{\sum (w|F_o|^2)^{1/2}} \times 100 \text{ for } [I < 2\sigma(I)].$$

Table 6. Data Collection Parameters for **11** and **12**

	11	12
chemical formula	C ₇₂ H ₈₄ K ₄ O ₈	C ₈₆ H ₈₂ K ₄ N ₆ O ₄
fw	1233.79	1419.98
temp (K)	168(2)	168(2)
space group	orthorhombic <i>Aba2</i>	tetragonal <i>P4</i>
<i>a</i> (Å)	18.178(3)	28.2270(13)
<i>b</i> (Å)	19.511(3)	28.2270(13)
<i>c</i> (Å)	19.055(3)	9.7046(4)
α (deg)	6758.3(17)	7732.3(6)
β (deg)	4	4
γ (deg)	1.213	1.220
<i>V</i> (Å ³)	0.316	0.284
<i>Z</i>	3.53	5.55
<i>D</i> _{calcd} (Mg/m ³)	9.36	11.09

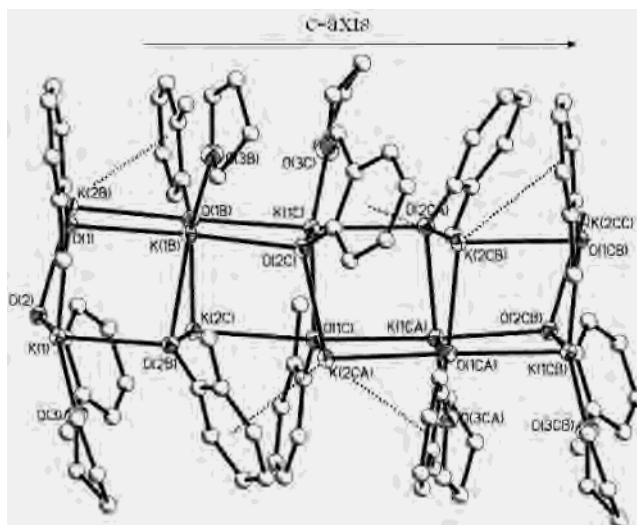
$${}^a R1 = \frac{\sum ||F_o| - |F_c||}{\sum |F_o|} \times 100. {}^b wR2 = \frac{[\sum w(F_o^2 - F_c^2)^2]}{\sum (w|F_o|^2)^{1/2}} \times 100 \text{ for } [I < 2\sigma(I)].$$

within the cell. The hydrogen atoms were fixed in positions of ideal geometry and refined within the XSHLL software.

Results and Discussion

The lack of structurally characterized K(OAr) led us to undertake the synthesis and characterization of a series of sterically varied 2,6-phenoxy derivatives. These ligands were selected due to their ability to alter the steric bulk around the metal center and our previous success in identifying the family of “Li(OAr)(solv)” compounds.¹⁸ The only simple, structurally characterized K(OAr) that we found in the literature was the phenoxide (OPh) derivative, characterized as [K(OPh) \cdot *n*HOPh]_∞ using powder diffraction data. This polymeric species, isolated from toluene, displays π -interactions between the aryl rings of the OPh ring and the neighboring K atoms.²³ For our system, stoichiometric attempts to generate a family of K(OAr) derivatives from toluene yielded only insoluble white precipitates. Since the soluble OPh species involved coordination of a Lewis base (i.e., H–OPh), we decided to also use stronger Lewis bases to reduce oligomerization.

Previously, we have reported that the use of strong Lewis bases, such as THF and py, have allowed for the crystallization of the “Li(OAr)(solv)” family of compounds.^{18,29} For these systems, whenever THF or py was added to the reaction mixture, the solubility of the product increased, and the

**Figure 1.** Thermal ellipsoid plot of **1**. Thermal ellipsoids are drawn at the 30% level.

appropriate solvent was found bound to the metal. The following details the syntheses and structures of a series of sterically varied potassium 2,6-phenoxy derivatives synthesized in both THF and py.

Synthesis. The alcoholysis of the KNR₂ was used as the general route to these K(OAr) derivatives (eq 2). This route was chosen due to the clean products isolated, the availability of starting materials, and its proven utility in the synthesis of the [Li(OAr)(solv)]_n adducts.¹⁸ Crystals were isolated for each reaction and structures shown to be {[K(μ -oMP)(THF)][K(μ -oMP)]₅∞} (**1**), {[K(η ⁶, μ -oMP)₄(η ⁶, μ -oMP)₂(py)₄][K(η ⁶, μ -oMP)₆(η ⁶-py)₄]}∞ (**2**), [K(μ -oPP)]₄(THF)₃ (**3**), {K₄(η ⁶, μ -oPP)₂(μ -oPP)₂(py)₃}∞ (**4**), [K(μ -oBP)(THF)]₆ (**5**), {K₆(η ⁶, μ -oBP)₂(μ -oBP)₄(py)₄}∞ (**6**), {K₃(η ⁶, μ -DMP)₂(μ -DMP)(THF)}∞ (**7**), {[K(η ⁶, μ -DMP)(py)]₂}∞ (**8**), {K(η ⁶, μ -DIP)}∞ (**9**), {K(η ⁶, μ -DBP)}∞ (**10**), [K(μ -DPE)(THF)]₄ (**11**), and [K(μ -DPE)(py)]₄·py₂ (**12**). These are shown in Figures 1–12, respectively.

The FTIR spectra of **1–12** show no stretches associated with OH or N(SiMe₃)₂ ligands, which is indicative of complete substitution by the alcohol–amine exchange (eq 1). The standard alkyl and aryl stretches for the aryloxide are present in each sample with small variations based upon the ring substitution. The IR spectra of **9** or **10** crystallized out of THF or py are identical independent of the solvent used. This is consistent with the solid-state structural determination. Due to the complexity of the M–O region, it was not possible to definitively assign a K–O stretch.

The volatility of coordinated solvent was previously noted for the lack of suitable elemental analyses of [Li(OAr)(solv)]_n. Elemental analyses for the potassium derivatives were not consistent for any of the solvated species (**1–8**, **11**, **12**); however, the unsolvated polymers (**9** and **10**) had elemental analyses that were in agreement with the solid-state structures. Therefore, the inconsistencies in the elemental analysis are most likely associated with preferential loss of solvent during analysis.

(29) Boyle, T. J.; Alam, T. M.; Peters, K. P.; Rodriguez, M. A. *Inorg. Chem.* **2002**, *40*, 6281.

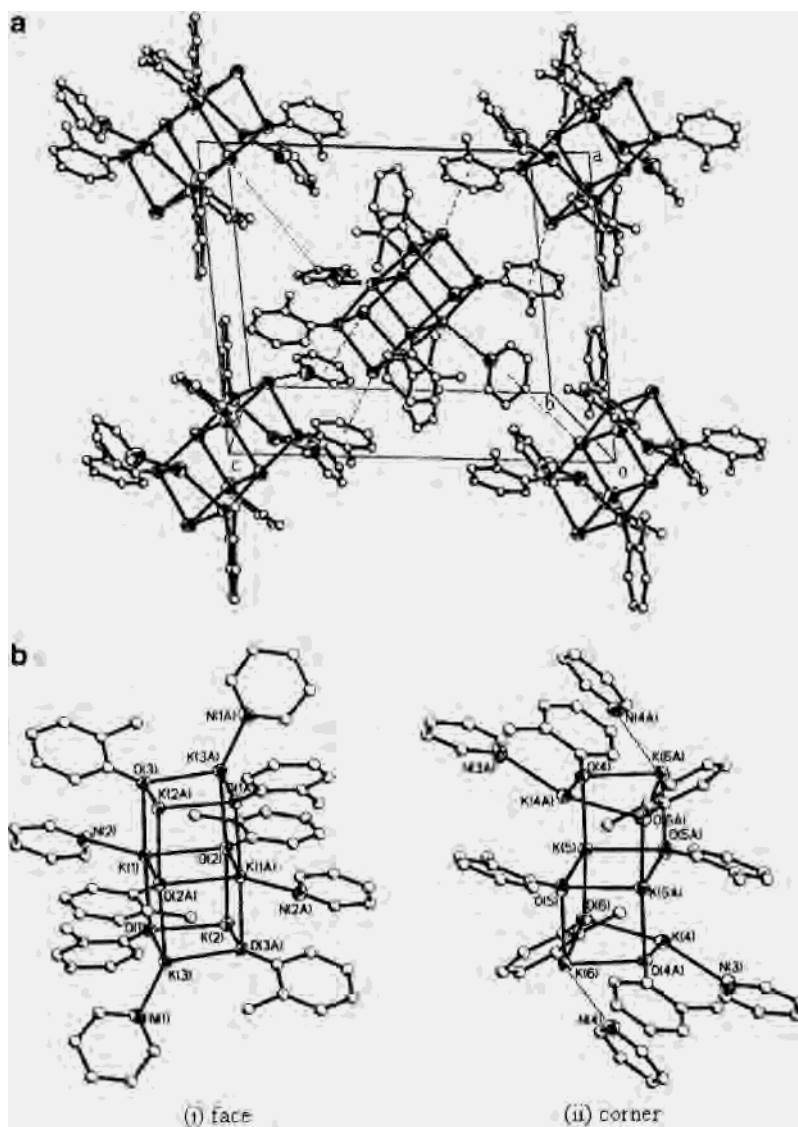


Figure 2. (a) Thermal ellipsoid plot of **2**. Thermal ellipsoids are drawn at the 30% level. (b) Individual components of unit cell: (i) face molecule, (ii) corner molecule.

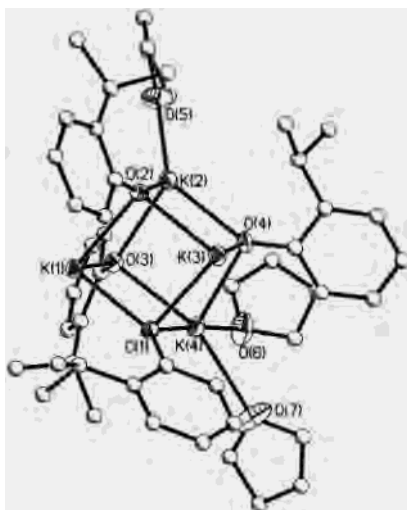


Figure 3. Thermal ellipsoid plot of **3**. Thermal ellipsoids are drawn at the 30% level.

Solid-State Structures. Tables 1–6 list the data collection parameters for **1–12**, tabulated by ligand. Figures 1–12

show the thermal plots of **1–12**, respectively. Full crystallographic data can be found in the Supporting Information. These compounds crystallized in a variety of space groups with $P\bar{1}$ the most frequently solved. In general, there were no molecules of solvent found in the crystal lattice, and only for the smaller ligands were the Lewis basic solvents found bound to the metal center. Some of these molecules actually use the π -system of the py to fill coordination sites on the K metals. For the bulkier ligands, polymeric chains were isolated without the coordination of solvent. The molecules range from hexagons to cubes to ladders to chains. The $K(\text{OAr})$ molecules observed are often best described as cubes of $[\text{K}-\text{OAr}]_4$ with various pieces missing (e.g., edges, corners), and this descriptor will be used throughout this discussion where appropriate.

Compound **1**, shown in Figure 1, was crystallized from THF and consists of four edge-missing, face-shared cubes forming a distorted tube of K and O atoms of general formula $\{([\text{K}(\mu_4\text{-oMP})(\text{THF})][\text{K}(\mu_3\text{-oMP})]_5)\}_\infty$. The missing edge alternates from back-basal to front-basal to front-apex

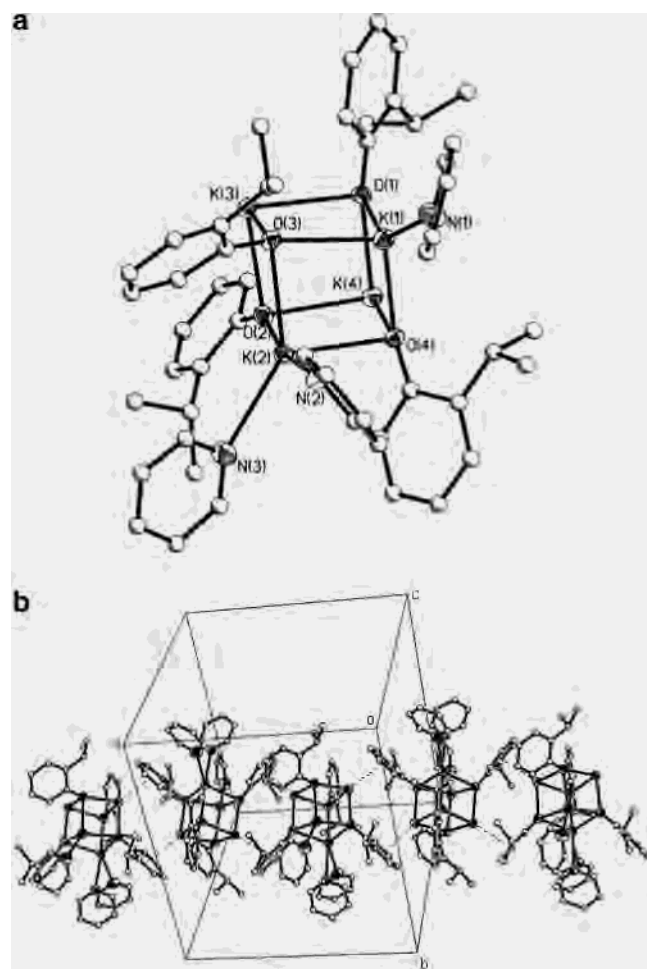


Figure 4. (a) Thermal ellipsoid plot of 4. Thermal ellipsoids are drawn at the 30% level. (b) Interaction between molecules shown along the *a*-axis.

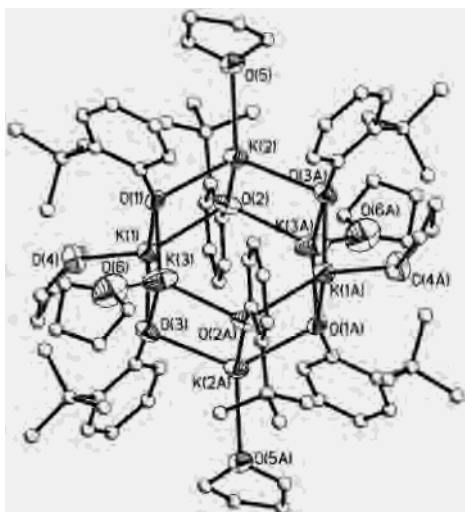


Figure 5. Thermal ellipsoid plot of 5. Thermal ellipsoids are drawn at the 30% level.

and then to the back-apex. The alternating K atoms in the tube bind a THF solvent molecule to generate a distorted 4-coordinate irregular (IRR) geometry but, through a π -interaction between unit cell moieties, adopt a trigonal bipyramidal (TBP) geometry. The remaining K atoms are 3-coordinated forming a formally pyramidal (PYD) geom-

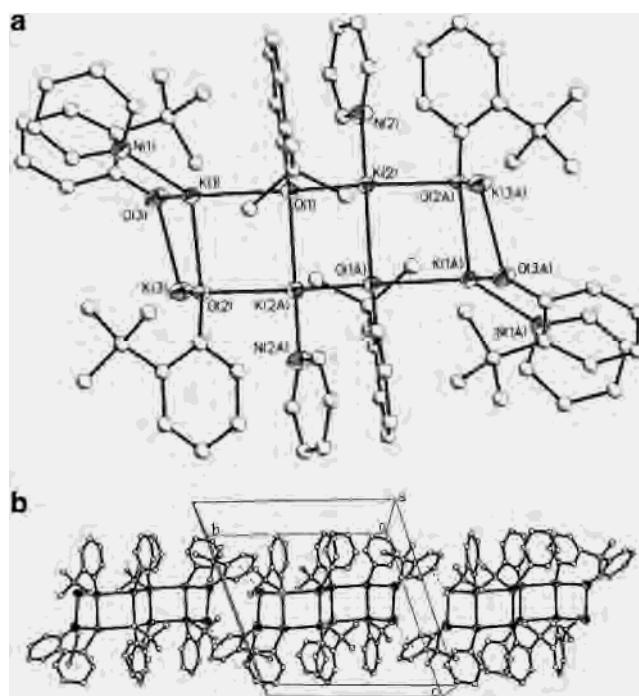


Figure 6. (a) Thermal ellipsoid plot of 6. Thermal ellipsoids are drawn at the 30% level. (b) Interaction between molecules shown along the *c*-axis.

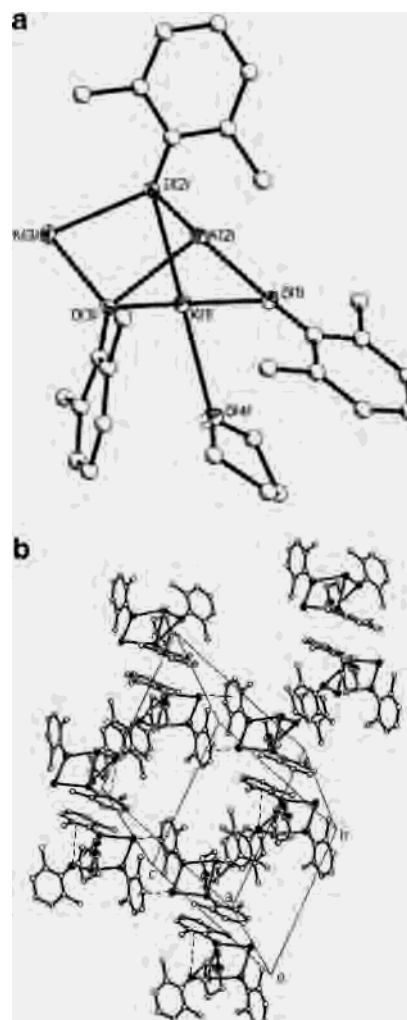


Figure 7. (a) Thermal ellipsoid plot of 7. Thermal ellipsoids are drawn at the 30% level. (b) Interaction between molecules shown along the *b*-axis.

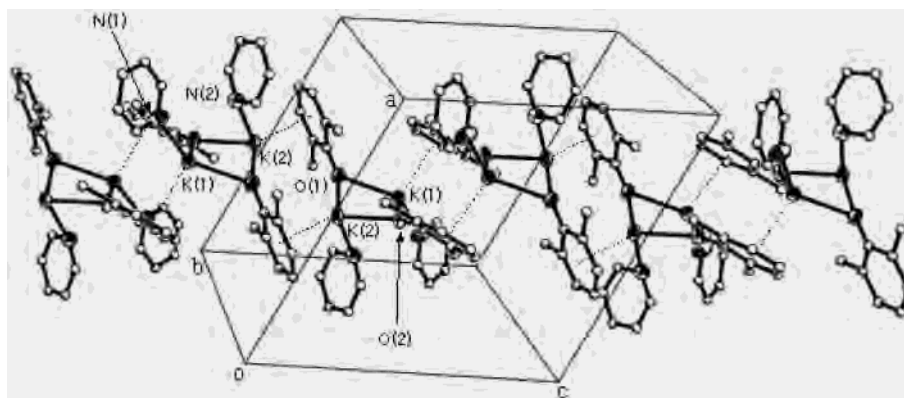


Figure 8. Thermal ellipsoid plot of **8**. Thermal ellipsoids are drawn at the 30% level.

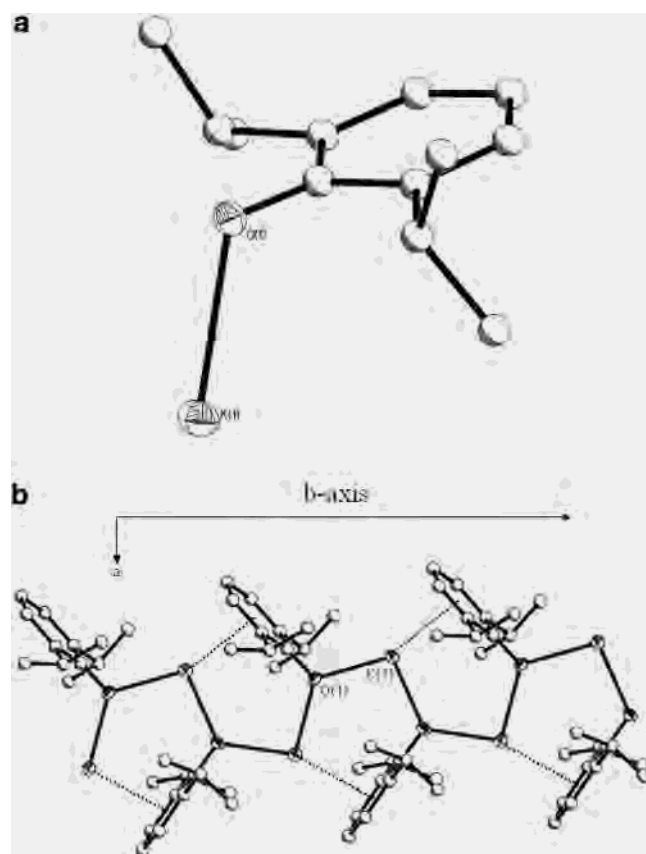


Figure 9. (a) Thermal ellipsoid plot of **9**. Thermal ellipsoids are drawn at the 30% level. (b) Interaction between molecules.

etry. Each of the aryloxide ligands act as a μ_3 -oMP ligand with the π -interaction of the ring coordinating with the K atoms that are 3-coordinated.

Smaller oligomers were found to form in py as observed for $\{[K_6(\eta^6\text{-}\mu_3\text{-oMP})_4(\eta^6\text{-}\mu_4\text{-oMP})_2(\text{py})_4] \cdot [K_6(\eta^6\text{-}\mu_3\text{-oMP})_6(\eta^6\text{-py})_4]\}_\infty$, **2**. The structure of **2** (Figure 2) has two unique molecules per unit cell, arranged on the face (Figure 2b, part i) and the corner (Figure 2b, part ii) of the unit cell. The face molecules consist of two face-shared cubes yielding $[K_6(\text{oMP})_6(\text{py})_4]$ stoichiometry. There are three types of K atoms: K(1) adopts a formally TBP geometry, K(2) adopts a PYR geometry with the oMP ligands, but there is an additional π -interaction which yields a distorted tetrahedral (Td) geometry, and K(3) is in a very distorted Td geometry.

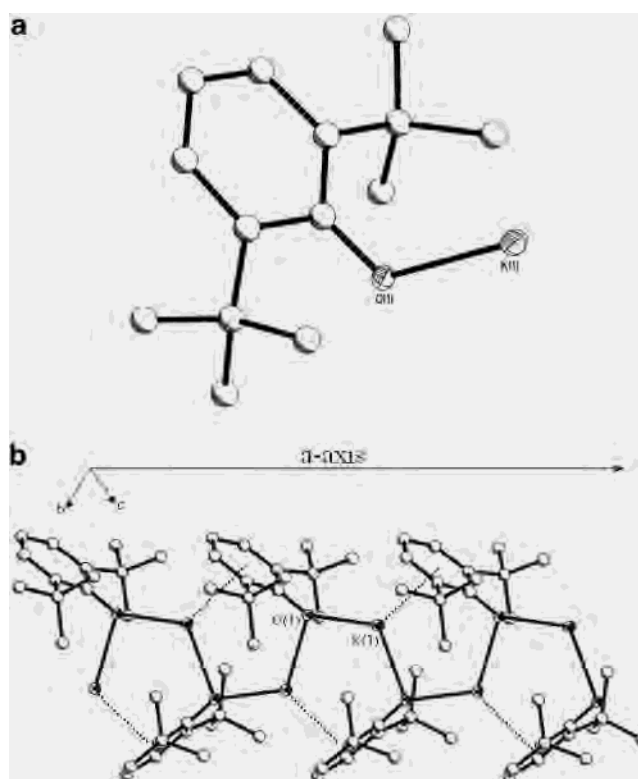


Figure 10. (a) Thermal ellipsoid plot of **10**. Thermal ellipsoids are drawn at the 30% level. (b) Interaction between molecules shown along the *a*-axis.

The corner species are similar to the face molecules but adopt a face-shared–opposite-edge-missing arrangement. Again, there are three types of K atoms: K(4) adopts an unusual T-shaped geometry, and K(5) and K(6) are both in IRR geometries that are converted to TBP through π -interactions. The stronger Lewis basic py molecules of **2** bind to a greater extent than the THF molecules of **1**. This allows for smaller oligomers to form, and discrete corner and facial molecules are observed in contrast to the polymeric species observed for **1**. However, the large radius to small charge ratio allows for intermolecular bonding, even for the saturated species of **2**.

In contrast, by using the oPP ligand which has a propyl group in the *ortho* position, the formation of face-shared cubes observed for **2** was inhibited, and a discrete cube was isolated as **3** (Figure 3). This must be attributed to the significant increase in the steric bulk of the oPP ligand in

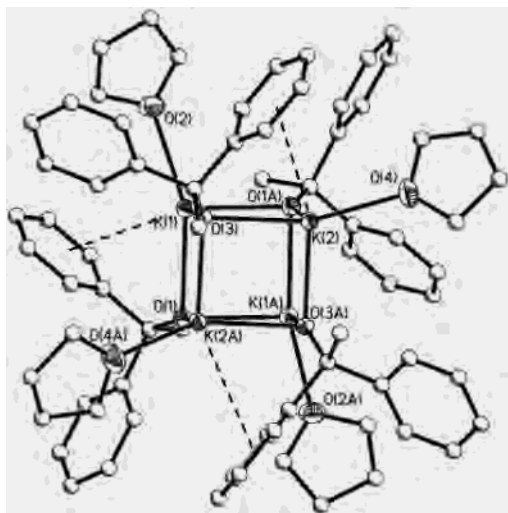


Figure 11. Thermal ellipsoid plot of **11**. Thermal ellipsoids are drawn at the 30% level.

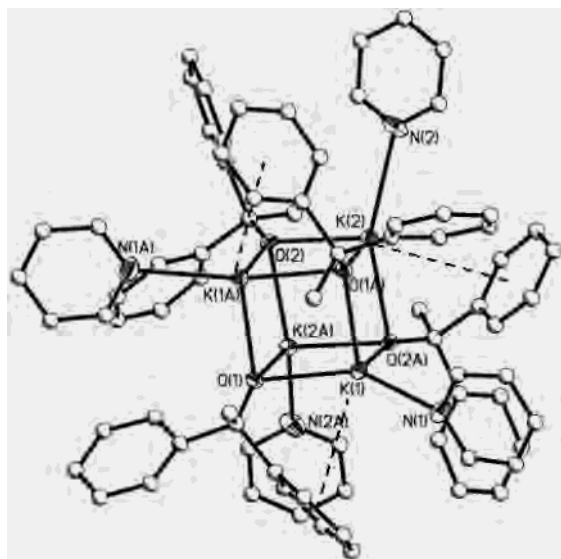


Figure 12. Thermal ellipsoid plot of **12**. Thermal ellipsoids are drawn at the 30% level.

comparison to oMP. Interestingly, two of the four K atoms of **3** are 3-coordinated without any association with the Lewis basic THF solvent molecules. The remaining K atoms are 4- and 5-coordinated, binding one and two THF molecules, respectively, resulting in an asymmetric molecule. The 3-coordinated K atoms are PYR in geometry but convert to distorted Td through an interaction with the π -ring of the oPP ligands of neighboring molecules. The asymmetric solvent binding was initially thought to be an anomaly; however, the identical structure (Figure 4) and intermolecular interaction were noted for the py adduct **4** (Figure 4a). This intermolecular interaction was never observed for the “Li(OAr)(solv)” family of compounds. Typically, the cube structures isolated were fully solvated, preventing such interactions. For those molecules partially solvated, the remaining Li atoms were sterically blocked by the OAr ligands, preventing any interactions.¹⁸ This must be associated with the smaller size of the Li versus K cations.³⁰

In contrast to the Li family of compounds, additional steric bulk does not lead to compounds¹⁸ of lower nuclearity, but instead, by adding the oBP ligand (*tert*-butyl group in the *ortho* position), a compound with a hexagon structure was isolated as **5** (Figure 5) wherein all of the K metal centers adopt very distorted Td geometries. This structural arrangement was also observed for [Li(OPh)(THF)]₆.¹⁰ By switching to the more polar py solvent but maintaining the oBP ligand set, a ladder like structure is observed for **6** (Figure 6). Four of the six potassium atoms are Td arranged, coordinated by bridging μ_3 -oBP ligands and coordinating py solvent molecules. The opposite terminal K atoms do not coordinate py but instead link to the next molecule by a π -interaction with the neighboring oBP rings (Figure 6a). This forms a polymeric chain of ladderlike “K(OAr)(py)” molecules.

Proceeding to the di-*ortho*-substituted ligands yielded additional unique molecular arrangements in comparison to the Li(OAr)(solv) complexes.¹⁸ The unusual nature of K(DMP), **7**, consists of three K atoms bridged equally by two μ_3 -DMP ligands and an additional μ -DMP ligand (Figure 7). This asymmetric arrangement leaves one of the K atoms 4-coordinated IRR by binding a THF molecule, a second K atom 3-coordinated with PYR geometry, and the final K atom only 2-coordinated with bent geometry. Again, π -bonding through the DMP aryl rings of a neighboring molecule (Figure 7a) fills the coordination sphere of the 2-coordinated K atom. For the py adduct, **8** was isolated and is shown in Figure 8. For this compound, each K is bound to two μ -DMP ligands and one py solvent molecule, forming a dinuclear subunit. A further π -interaction between the μ -DMP of one subunit and the K of the neighboring one yields distorted Td geometries for the K atoms.

Independent of the solvent used, the DIP derivative yielded **9** (Figure 9) which consists of the simple polymeric chain of alternating K atoms and DIP ligands with no observable coordination of solvent. There are some π -interactions to assist in fulfilling the coordination sphere of the K atoms (Figure 9a). Increasing the steric bulk to the DBP ligand yields **10** (Figure 10) which has the same basic structural arrangement as noted for **9** (see Figure 10a). For both structures, the K atoms are in a bent geometry but through the π -interaction of the aryloxide adopt a TRI geometry.

Further exploring the degree of π -coordination that these compounds will undergo, we investigated the diphenyl ethoxide (DPE) ligand. In THF, a standard cube was observed in the isolation of **11**, [K(DPE)(THF)]₄, shown in Figure 11. The same general structure was noted for the py adduct **12**, [K(DPE)(py)]₄, shown in Figure 12. The displacement of the rings away from the metal center by a single methine group apparently reduces the steric hindrance of the ligand around the metal center. This reduction is enough to allow solvent to bind. This solvation eliminates the necessity of π -binding through neighboring OAr rings. However, there appears to be some π -interaction between the DPE phenyl rings and neighboring K atoms of the same molecule. The metal centers in each of these structures possess very

(30) Shannon, R. D. *Acta Crystallogr.* **1976**, A32, 751.

distorted Td geometries but, due to this π -interaction, adopt TBP geometries.

There are some general variations noted for the “K(OAr)(solv)” compounds in comparison to the “Li(OAr)(solv)” species.¹⁸ In particular, not all of the K compounds bind solvent. Furthermore, polymer chains were reported for the K, whereas for the Li analogues only molecular species were observed. This was similar to what was observed for the “ATi(OR)₅” species wherein the Li formed discrete molecules but the larger congeners formed chains.¹⁷ This phenomenon was attributed to the size of the alkali metal cations. Finally, π -interactions were observed between the K atoms and phenyl rings of the aryloxide ligands, an interaction not observed in the Li systems.¹⁸

Solution-State NMR. In an effort to understand the solution behavior of these compounds, crystalline material of each sample was dissolved in its parent solvent. These solvents were chosen in an attempt to maintain structural integrity and ensure solubility. Solution samples were made as concentrated as possible and stored in sealed NMR tubes. We attempted to collect ³⁹K NMR spectral data; however, the signal-to-noise ratio and the extremely broad signals did not allow for meaningful data to be collected. Therefore, only ¹H and ¹³C{¹H} data were reported.

The ¹H NMR data yielded very limited information concerning solution structures. For the THF ligated species (**1**, **3**, **5**, **7**, **11**) and the py ligated compounds (**2**, **4**, **6**, **8**, **12**), only the resonances associated with the presence of the appropriate ligands could be discerned. The NMR spectra of the polymeric unsolvated species, **9** and **10**, were collected in both solvents. For each sample, only one ligand set was present, indicating that the solid-state structures for the majority of these species are disrupted in solution either through reduction of the oligomerization or equalization of the solvation of the various K atoms. Since the smaller components are merely π -interacting with the other systems, equation of the smaller units through solvent incorporation seems more appropriate than complete disruption of the complex molecules formed. Additional information could be gained through the redissolution of these compounds in a nonparent solvent. However, the low solubility and complex behavior greatly limit any solution information that can be garnered by this approach. Molecular weight determinations were not undertaken due to the low solubility in appropriate solvents for this methodology.

Summary and Conclusion

A family of “K(OAr)(solv)” species (**1–10**) has been structurally characterized for the first time which may add to the interpretation of such processes as the carboxylation of alkali-phenolates (i.e., Kolbe–Schmidt process). In comparison to the structures reported for the “Li(OAr)(solv)” system, there is less systematic variation for the K system. The K(OAr) structures range from cubes to hexagons to polymeric chains of different arrangements. The majority of these compounds are polymeric, using the π -electrons of the aryl ring to fill coordination spheres of neighboring K atoms. The K atoms of the less sterically hindering aryloxide ligands (oMP, oPP, oBP, and DMP) allow for solvent coordination, resulting in a Td geometry. The K atoms that use the more sterically hindering ligands (DIP and DBP) are PYD without coordination of solvent. The smallest and most sterically hindering species form polymeric species whereas the intermediate sterically demanding species form discrete molecules. To generate the intermolecular π -interaction observed for the aryloxides, the phenyl rings must be closely associated with the K atoms. Any additional separation leads to simple solvated cube structures with only intramolecular π -interactions, as evidenced by the DPE ligated species (**11–12**). The solid-state structures of **1–12** do not appear to be retained in solution due to the simplicity of the resulting NMR spectra. Clearly, **1–12** do not represent the only possible structures for this system; effects from concentration and temperature, as well as subtle variations in handling techniques, will likely produce several variants of the structures reported here. Continued work involving additional congeners will be explored to further understand the structures of the alkali metal phenoxy derivatives.

Acknowledgment. For support of this research, the authors would like to thank the Office of Basic Energy Science of the Department of Energy and the United States Department of Energy. Sandia is a multiprogram laboratory operated by Sandia Corporation, a Lockheed Martin Company, for the United States Department of Energy under Contract DE-AC04-94AL85000.

Supporting Information Available: X-ray crystallographic files in CIF format for the structures **1–12** are available. This material is available free of charge via the Internet at <http://pubs.acs.org>.

IC034222K